Reduction of Cobalt and Iron Corroles and Catalyzed Reduction of CO_2

Jan Grodkowski[†] and Pedatsur Neta*

Physical and Chemical Properties Division, National Institute of Standards and Technology, Gaithersburg, Maryland 20899-8381

Etsuko Fujita*

Chemistry Department, Brookhaven National Laboratory, Upton, New York 11973

Atif Mahammed, Liliya Simkhovich, and Zeev Gross*

Department of Chemistry and Institute of Catalysis Science and Technology, Technion—Israel Institute of Technology, Haifa 32000, Israel

Received: October 1, 2001; In Final Form: January 30, 2002

The role of cobalt and iron corroles in catalytic CO_2 reduction has been studied. Chemical, electrochemical, and photochemical reductions of the stable metal corroles Ph_3PCo^{III}(tpfc) (tpfc = 5,10,15-tris(pentafluorophenyl)corrole), $ClFe^{IV}$(tpfc), and $ClFe^{IV}$(tdcc) (tdcc = 5,10,15-tris(2,6-dichlorophenyl)corrole) have been carried out in acetonitrile solutions. Stepwise reduction to the $[M^{II}(tpfc)]^-$ and $[M^{I}(tpfc)]^{2-}$ states was observed in all cases. Gradual reduction with sodium amalgam permitted recording of the optical absorption spectra of the various oxidation states and showed that the M^I state reacts with CO_2. Cyclic voltammetry in Ar-saturated acetonitrile solutions permitted determination of the following half-wave potentials: for Ph_3PCo^{III}(tpfc), 1.11 V, 0.72 V, −0.42 V (E_{pc}), −1.44 V, −2.3 V (E_{pc}); for $ClFe^{IV}$(tpfc), 0.44 V, −1.01 V (E_{pc}), −1.60 V, −2.2 V (E_{pc}); for $ClFe^{IV}$(tdcc), 0.24 V, −1.18 V (E_{pc}), −1.78 V vs SCE with a scan rate of 0.1 V s^{-1}. Cyclic voltammetry in CO_2-saturated solutions indicated that the Co^I and Fe^I complexes react with CO_2 and that the reduced Fe(tdcc) complex is the most efficient electrocatalyst for CO_2 reduction, showing the largest catalytic currents among these corroles. Photochemical reduction in CO_2-saturated acetonitrile solutions containing *p*-terphenyl (TP) as a sensitizer and triethylamine (TEA) as a reductant led to production of CO and H_2. These experiments also show that Fe(tdcc) is more effective than the other corroles as a CO_2 reduction catalyst. The present finding that the M^I oxidation states of the cobalt and iron corroles can react with CO_2 is in contrast with the case of the respective porphyrins and phthalocyanines, which do not react with CO_2 until they are reduced beyond the M^I state.

Introduction

Several transition metal complexes are known to act as electron-transfer mediators for photochemical[1,2] or electrochemical[3] reduction of CO_2.[4] Recent studies have shown that iron and cobalt porphyrins (MP) are effective homogeneous catalysts for the electrochemical[5] and photochemical[6,7] reduction of CO_2 to CO and formic acid. A more recent study has shown that Fe and Co phthalocyanines also catalyze photoreduction of CO_2 in homogeneous solutions.[8] With both porphyrins and phthalocyanines it was found that the $[M^IP]^-$ complexes do not react with CO_2 and that the products of the next reduction step are the reactive species. These products were formulated as zerovalent metalloporphyrins $[M^0P]^{2-}$ and monovalent cobalt phthalocyanine radical anion $[Co^IPc^\bullet]^{2-}$. The present study is aimed at characterizing the species produced by reduction of cobalt and iron corroles and examining their role in photochemical reduction of CO_2. Corroles lack one meso bridge and thus have a smaller macrocycle cavity than porphyrins. Their four nitrogens bear three protons, as compared with two protons in porphyrins. For these reasons, corroles stabilize the metal center at a higher oxidation state than porphyrins. On the basis of their behavior in oxidation reactions,[9,10] it is expected that their reduction reactions will take place at more negative potentials than the corresponding reactions of metalloporphyrins. If the reduction to the M^I state occurs at a very negative potential the M^I corrole may react with CO_2. Therefore, chemical, electrochemical, and photochemical methods were used to study the reduction reactions of several corroles and their interaction with CO_2.

Experimental Section

The cobalt corrole was synthesized as the triphenylphosphine complex, Ph_3PCo^{III}(tpfc) (tpfc is the trianion of 5,10,15-tris-(pentafluorophenyl)corrole) and the iron corroles as the chloride complexes, $ClFe^{IV}$(tpfc) and $ClFe^{IV}$(tdcc), as described before.[11,12]

Triethylamine (TEA) was obtained from Aldrich and was refluxed over sodium and distilled under nitrogen. Acetonitrile (MeCN) used as solvent for sodium amalgam reduction was purified by published methods[13] and stored in a vacuum over activated molecular sieves. Dried and distilled MeCN was used

* Corresponding authors.
[†] On leave from the Institute of Nuclear Chemistry and Technology, Warsaw, Poland.

10.1021/jp013668o CCC: $22.00
Published on Web 04/06/2002

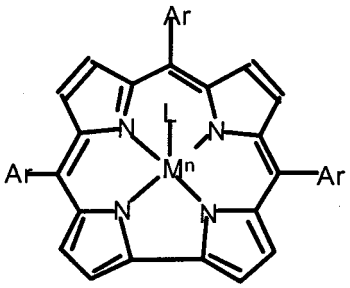

M	n	Ar	L	Abbreviation
Co	III	C_6F_5	Ph_3P	Ph_3PCo(tpfc)
Fe	IV	C_6F_5	Cl	ClFe(tpfc)
Fe	IV	2,6-$C_6H_3Cl_2$	Cl	ClFe(tdcc)

for electrochemical experiments and dry spectrograde MeCN was used for photochemical experiments. All experiments were performed at room temperature, (22 ± 2) °C.

Cyclic voltammetry measurements were carried out with MeCN solutions containing 0.5 mmol L^{-1} of the metal corrole and 0.05 mol L^{-1} Bu_4NPF_6 as the electrolyte, with scan rates ranging from 10 mV s^{-1} to 10 V s^{-1}. A conventional three-electrode system consisting of a glassy carbon working electrode, a Pt counter electrode, and a standard calomel reference electrode was used with a BAS100B electrochemical analyzer. Ferrocene ($E_{1/2}$ = 0.39 V vs SCE) was added as an internal standard at the end of all experiments. All potentials are given with reference to the standard calomel electrode. A glassy carbon electrode was polished before each scan and several scans were taken at different ranges of potential to determine the various reversible reduction and oxidation steps.

The UV−vis spectra of reduced corroles were recorded in MeCN solutions following stepwise reduction of Ph_3PCo^{III}(tpfc), $ClFe^{IV}$(tpfc), and $ClFe^{IV}$(tdcc) by sodium amalgam (0.5% Na in Hg) in sealed glassware equipped with an optical cell. The solution was exposed to the sodium amalgam for a few seconds and then returned to the optical cell compartment and its spectrum was recorded. The process was repeated many times and the end point of each reduction was carefully monitored by the loss of isosbestic points.

Photochemical experiments were performed with a 300-W xenon lamp, using water filters to absorb the IR and Pyrex filters to absorb the UV (λ < 310 nm). Solutions were placed in an irradiation cell equipped with a water cooling system to maintain the solution temperature, were bubbled with He or CO_2, and then were photolyzed. For recording of optical absorption spectra before and after photolysis, the solution was irradiated in a quartz optical cell, with 2 mm or 10 mm optical path length, attached to a quartz tubing and sealed with a septum. For analysis of the gases evolved, 35 mL of the solution was placed in a 43 mL Pyrex bulb cooled by a water jacket, saturated with the required gas, and then photolyzed. After various intervals, the headspace was analyzed for CO and H_2 by gas chromatography (Carboxen-1000 column, thermal conductivity detector). The total amounts of these gases in both solution and gas phase were calculated from the known solubilities and are reported as concentration as if all the gases remained in the photolyzed solution.

Results and Discussion

Electrochemical Reduction of the Corroles. The results of cyclic voltammetry measurements with Ph_3PCo^{III}(tpfc), $ClFe^{IV}$(tpfc), and $ClFe^{IV}$(tdcc) are summarized in Table 1. Ph_3PCo^{III}(tpfc) undergoes two reversible one-electron oxidations at $E_{1/2}$ = 0.72 and 1.11 V in MeCN under an Ar atmosphere. The first reduction is irreversible and occurs at E_{pc} = −0.42 V at a scan rate of 0.1 V s^{-1} and this reduction is coupled to reoxidation peaks at E_{pa} = −0.3 and 0 V (Figure 1). This reduction is assigned to $Co^{III\rightarrow II}$ and the irreversibility is due to a partial loss of the Ph_3P ligand from $[Ph_3PCo^{II}(tpfc)]^-$. The second reduction (most likely $Co^{II\rightarrow I}$) is reversible and takes place at −1.44 V. The third reduction is irreversible and occurs at −2.3 V at a scan rate of 0.1 V (Figure 1, dashed line). The third reduction may be a multiple-electron reduction of the fluorinated phenyl rings. Kadish et al.[9a] reported that Ph_3PCo(omc) (where omc = 2,3,7,8,12,13,17,18-octamethylcorrole) has oxidation potentials of 0.19, 0.76, and 1.54 V, and reduction potentials of −0.86 (E_{pc}) and −1.92 V in PrCN. The potentials of Ph_3PCo^{III}(tpfc) are all shifted by about 0.35 V to 0.50 V toward the positive direction compared to Ph_3PCo(omc) due to electron withdrawing effects of the fluorinated phenyl rings. A similar difference is found when comparing the reduction potentials of a series of other metal complexes of tpfc and omc,[14] as well as the Co complexes of tetrakis(perfluorophenyl)porphyrin[7] and octaethylporphyrin.[15]

In the presence of CO_2, the wave for the $Co^{III\rightarrow II}$ reduction is practically the same as those in the presence of Ar at any scan rate, while the wave for the $Co^{II\rightarrow I}$ shows slightly increased current for reduction but no current for reoxidation at scan rates of 20 to 100 mV s^{-1} (Figure 1, dotted line). The changes in the

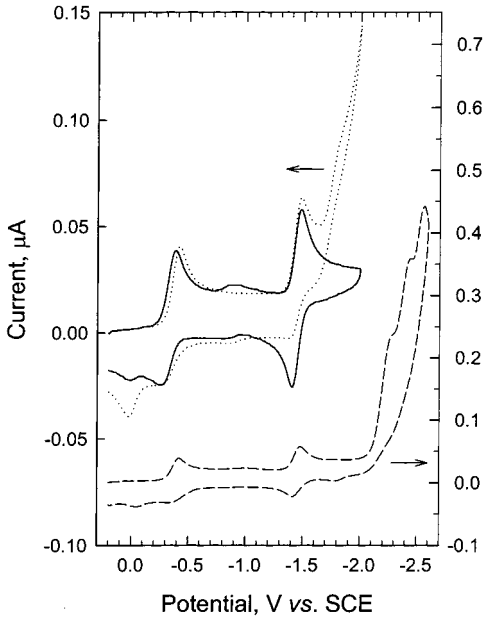

Figure 1. Cyclic voltammograms of Ph_3PCo^{III}(tpfc) in MeCN solutions saturated with Ar (solid line) and with CO_2 (dotted line), scanned between +0.2 V and −2.0 V vs SCE. A wider scan of the Ar-saturated solution between +0.2 V and −2.6 V is shown by the dashed line. Scan rate 0.1 V s^{-1}.

TABLE 1: Half-Wave Potentials for Reduction of the Corroles in MeCN

corrole	$E_{1/2}$, V vs. SCE
Ph_3PCo^{III}(tpfc)[a]	−0.42[b], −1.44, −2.3[b]
$ClFe^{IV}$(tpfc)	0.44, −1.01[b], −1.60, −2.2[b]
$ClFe^{IV}$(tdcc)	0.24, −1.18[b], −1.78

[a] Oxidation took place at $E_{1/2}$ 0.72 and 1.11 V. [b] E_{pc} at a scan rate of 0.1 V s^{-1}.

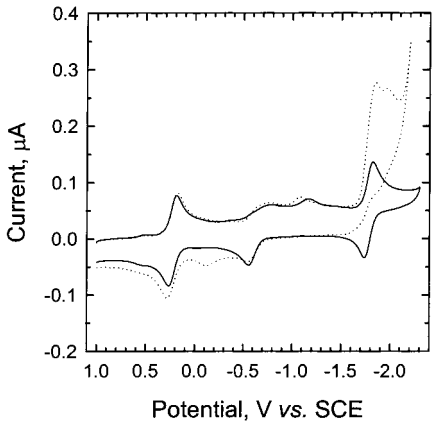

Figure 2. Cyclic voltammograms of $ClFe^{IV}$(tdcc) in MeCN solutions saturated with Ar (solid lines) and with CO_2 (dotted line). Scan rate 0.1 V s^{-1}.

$Co^{II\rightarrow I}$ peaks are more pronounced at lower scan rates and disappear upon increasing the scan rate to 5 V s^{-1}, indicating a slow reaction of $[Co^{I}(tpfc)]^{2-}$ with CO_2 (<50 L mol^{-1} s^{-1}). At more negative potentials, high catalytic currents are observed in the presence of CO_2.

$ClFe^{IV}$(tpfc) and $ClFe^{IV}$(tdcc) (Figure 2) show similar electrochemical behavior. $ClFe^{IV}$(tpfc) is reversibly reduced at $E_{1/2}$ = 0.44 V. Voltammograms at the narrow range of +1.0 V to −0.2 V show reversibility at a scan rates of 0.1 V s^{-1}, indicating that the Cl^- remains bound to the Fe^{III} product on the time scale of these experiments. The second reduction step is clearly irreversible at a scan rate of 0.1 V s^{-1}, indicating a loss of the Cl^- ligand during the reduction. The reduction of $[ClFe^{III}(tpfc)]^-$ takes place at E_{pc} = −1.01 V and is coupled to a reoxidation peak for Fe^{II}(tpfc) at E_{pa} = −0.43 V. The third reduction ($Fe^{II\rightarrow I}$) takes place reversibly at −1.60 V, and the fourth reduction occurs irreversibly at −2.2 V (E_{pc}) at a scan rate of 0.1 V. In the presence of CO_2, the wave for the $Fe^{II\rightarrow I}$ reduction shows increased current for reduction but no current for reoxidation at scan rates of 20 mV s^{-1} to 1 V s^{-1}. The wave becomes practically the same as that under an Ar atmosphere at a scan rate of 10 V s^{-1}. The reaction rate of $[Fe^{I}(tpfc)]^{2-}$ with CO_2 seems slightly faster than that of $[Co^{I}(tpfc)]^{2-}$. However, plots of the catalytic current vs $[CO_2]^{1/2}$ with Fe(tpfc) at scan rates of 10 mV s^{-1} and 20 mV s^{-1} do not show linear relationship over a wide range but rather indicate saturation at high $[CO_2]$.

$ClFe^{IV}$(tdcc) exhibits reduction potentials more positive (≈0.2 V) than $ClFe^{IV}$(tpfc). $ClFe^{IV}$(tdcc) is reversibly reduced at $E_{1/2}$ = 0.24 V and irreversibly reduced at E_{pc} = −1.18 V at a scan rate of 0.1 V s^{-1}. This reduction is coupled to a reoxidation peak at E_{pa} = −0.55 V. A small reduction step near −0.6 V is probably due to a small amount of Fe^{III}(tdcc) produced by partial loss of chloride following the first reduction. The third reduction ($Fe^{II\rightarrow I}$) takes place reversibly at −1.78 V (Figure 2, solid line). In the presence of CO_2, the wave for the $Fe^{II\rightarrow I}$ reduction shows increased current for reduction but no current for reoxidation at scan rates of 20 mV s^{-1} to 10 V s^{-1} (Figure 2, dotted line). At all scan rates, the ratio between the current under CO_2 and the current under Ar, $I(CO_2)/I(Ar)$, was the highest for this complex. For example, at a scan rate of 100 mV s^{-1} the ratio was 2.67 for Fe(tdcc), 1.67 for Fe(tpfc), and 1.05 for Co(tpfc). Thus, Fe(tdcc) is the best CO_2-reduction electrocatalyst among these corroles, probably due to its more negative reduction potential.

Reduction of the Corroles by Sodium Amalgam. The optical absorption spectra obtained during stepwise reduction

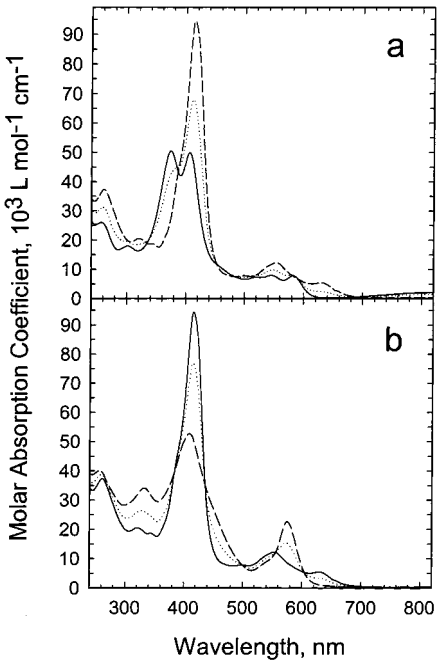

Figure 3. Absorption spectra recorded upon reduction of Ph_3PCo^{III}(tpfc) by sodium amalgam in MeCN solutions. (a) Reduction of Co^{III} to Co^{II}. (b) Reduction of Co^{II} to Co^{I}. In each case, the initial spectrum is the solid line, the intermediate spectra are the dotted lines, and the final spectrum is the dashed line.

of Ph_3PCo^{III}(tpfc) and $ClFe^{IV}$(tpfc) by sodium amalgam in MeCN solutions are shown in Figures 3 and 4, respectively. The optical absorption spectrum of $[(CO)Fe^{II}(tpfc)]^-$ is given in Figure 5. The UV−vis spectral data for all three corroles in their various oxidation states are summarized in Table 2.

The UV−vis spectra obtained in this study for Ph_3PCo^{III}(tpfc) and its first reduction product, $[Co^{II}(tpfc)]^-$ (Figure 3a), are somewhat similar to those reported for the Ph_3PCo^{III}(omc) and its reduced species.[9a] Figure 3b shows the second reduction. Since the spectrum of the product is only slightly shifted from that of $[Co^{II}(tpfc)]^-$ and exhibits no absorption in the near-IR, and by comparison with the case of similar cobalt porphyrins, we ascribe this product to $[Co^{I}(tpfc)]^{2-}$ rather than to the Co^{II} radical anion. Although this assignment is not solidly proven by the present results, we adopt this notation for the present article and will refer to both Co^{I} and Fe^{I} corroles.

On comparing the spectra of the starting materials, it is noticed that while Ph_3PCo^{III}(tpfc) exhibits two peaks in the Soret region with equal intensities (Figure 3a), Ph_3PCo^{III}(omc) exhibits mainly one Soret peak and a shoulder.[9a] Since the second peak in both cases is at the same wavelength as the intense peak of the Co^{II} complex, we initially suspected that the second peak of Ph_3PCo^{III}(tpfc) may be due to the presence of some Co^{II} complex in the starting materials.[16] However, when we attempted to oxidize an acetonitrile solution of this material at 0.6 V vs. SCE, we did not observe any significant current nor spectral change. Furthermore, Ph_3PCo^{III}(tpfc) has been shown to be pure by TLC and was found not to contain any paramagnetic impurities.[17] The possibility that the two peaks are due to two forms of the complex, resulting from partial dissociation of the Ph_3P ligand in solution, is ruled out since addition of a 1000-fold excess of Ph_3P did not change the spectrum.

The results for reduction of $ClFe^{IV}$(tpfc) in three distinct steps to $[Fe^{I}(tpfc)]^{2-}$ are shown in Figure 4 and indicate clean and

TABLE 2: Spectroscopic Properties of the Corroles in Acetonitrile Solutions[a]

corrole	λ_{max}, nm ($10^{-3}\,\epsilon$, L mol^{-1} cm^{-1})
Ph_3PCo^{III}(tpfc)	258 (24.8), 301 (17.5), 374 (50.0), 406 (49.9), 520 (7.4), 546 (8.1), 583 (8.0), 806 (2.4)
$[Co^{II}(tpfc)]^-$	264 (37.1), 322 (20.5), 412(>95), 498 (7.8), 522 (12.2), 630 (5.5)
$[Co^{I}(tpfc)]^{2-}$	260 (40.0), 332 (34.2), 408 (52.8), 574 (22.6)
$ClFe^{IV}$(tpfc)	370 (44.3), 394 (46.8), 606 (3.5)
Fe^{III}(tpfc)	326 (32.1), 406 (45.7), 532 (13.4), 706 (4.8)
$[Fe^{II}(tpfc)]^-$	304 (20.5), 410 (56.3), 426 (55.0), 476 (23.5), 526 (8.5), 594 (18.8)
$[COFe^{II}(tpfc)]^-$	403 (95.5), ~530 (11.9), 553 (12.4)
$[Fe^{I}(tpfc)]^{2-}$	423 (37.8), 472 (27.2), 622 (13.3), 782 (3.6)
$ClFe^{IV}$(tdcc)	360 (38.2), 394 (41.3), 500sh (8.1), 550sh (5.3), 600sh (3.7), 744 (1.3)
Fe^{III}(tdcc)	326 (29.7), 410 (44.8), 540 (13.6), 730 (5.3)
$[Fe^{II}(tdcc)]^-$	305 (21.5), 415 (54.1), 432 (51.1), 482 (22.7), 530 (10.5), 564sh (12.3), 604 (22.5)
$[COFe^{II}(tdcc)]^-$	406 (>100), 526sh (12.2), 560 (15.3)
$[Fe^{I}(tdcc)]^{2-}$	434 (36.9), 478 (24.6), 562 (11.5), 606 (15.0), 638sh (12.1), 776 (5.6)

[a] Molar absorption coefficients ϵ were calculated by assuming 100% conversion from starting materials. Their estimated standard uncertainties are ±10%.

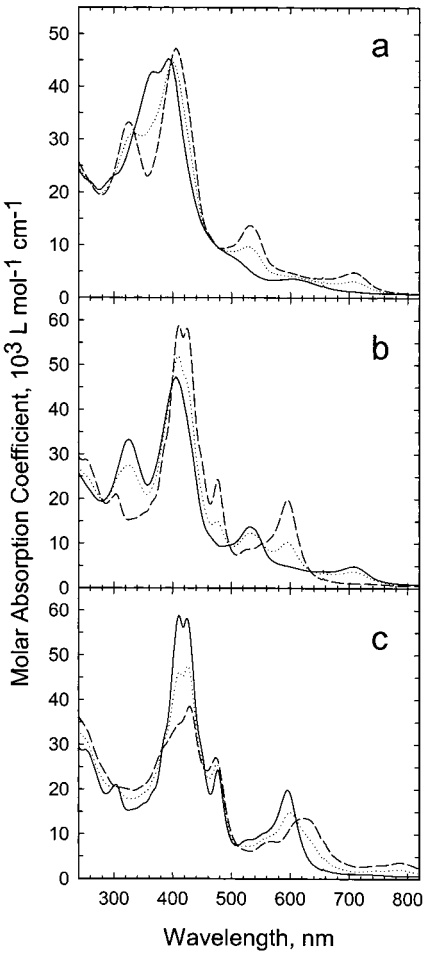

Figure 4. Absorption spectra recorded upon reduction of $ClFe^{IV}$(tpfc) by sodium amalgam in MeCN solutions. (a) $Fe^{IV} \rightarrow Fe^{III}$, (b) $Fe^{III} \rightarrow Fe^{II}$, (c) $Fe^{II} \rightarrow Fe^{I}$. In each case the initial spectrum is the solid line, the intermediate spectrum is the dotted line, and the final spectrum is the dashed line.

quantitative reduction in each step. Only the Fe^{II} corrole forms a strong complex with CO and its spectrum is shown in Figure 5. The Fe^{II} corrole for this experiment was produced by reduction with sodium amalgam or by photochemical reduction as described below.

Addition of CO_2 to the MeCN solutions of $[M^{I}(tpfc)]^{2-}$ resulted in a color change indicating formation of M^{II} complexes. The spectrum of the product obtained from $[Fe^{I}(tpfc)]^{2-}$ was a combination of the spectra of $[Fe^{II}(tpfc)]^-$ and a very small

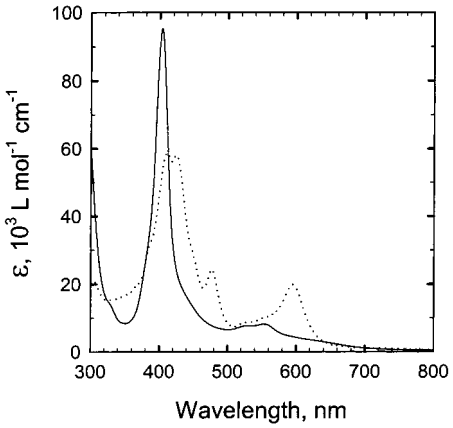

Figure 5. Absorption spectrum of $[COFe^{II}(tpfc)]^-$ in MeCN solutions containing 5% TEA (solid line) compared to the absorption spectrum of $[Fe^{II}(tpfc)]^-$ (dotted line).

fraction of $[(CO)Fe^{II}(tpfc)]^-$. We interpret these findings by the following reactions:

$$[M^{I}(tpfc)]^{2-} + CO_2 \rightarrow [(CO_2)M(tpfc)]^{2-} \quad (1)$$

$$[(CO_2)M(tpfc)]^{2-} + CO_2 \rightarrow M^{III}(tpfc) + CO + CO_3^{2-} \quad (2)$$

$$M^{III}(tpfc) + [M^{I}(tpfc)]^{2-} \rightarrow 2\,[M^{II}(tpfc)]^- \quad (3)$$

$$[Fe^{II}(tpfc)]^- + CO \leftrightarrows [(CO)Fe^{II}(tpfc)]^- \quad (4)$$

The $[M^{I}(tpfc)]^{2-}$ complexes react with CO_2 to form an adduct, which decomposes to CO and M^{III}(tpfc). This decomposition may be enhanced by CO_2, since no protons are available to accept the oxide. The subsequent reaction 3 must be fast to effect practically complete conversion of the corrole into $[M^{II}(tpfc)]^-$. This product does not react with CO_2 but, in the case of the iron complex, it can bind with CO to form an equilibrium mixture. A higher fraction of $[(CO)Fe^{II}(tpfc)]^-$ was obtained in the photochemical experiments and is discussed below, but the spectra for the cobalt complexes show no evidence for binding of CO to $[Co^{II}(tpfc)]^-$.

Photochemical Reduction of the Corroles. As in the earlier experiments with cobalt and iron porphyrins[7,18] and phthalocyanines,[8] the corroles were photoreduced in deoxygenated MeCN solutions containing triethylamine (TEA) (5 vol %, 0.36 mol L^{-1}) and *p*-terphenyl (TP) (0.03 to 3 mmol L^{-1}). The reason for the use of TP is that direct photochemical reduction of the M^{II} complexes by TEA is not efficient since there is no significant binding of TEA to the metal center. The use of

p-terphenyl as a sensitizer is based on the highly efficient formation of the *p*-terphenyl radical anion by reaction of the singlet excited state of TP with TEA,[19]

$$TP \xrightarrow{h\nu} TP^* \quad (5)$$

$$TP^* + Et_3N \rightarrow TP^{\bullet -} + Et_3N^{\bullet +} \quad (6)$$

and the rapid reduction of the metal complex by $TP^{\bullet -}$, which has a highly negative reduction potential (−2.45 V vs SCE in dimethylamine).[19]

$$TP^{\bullet -} + [M^{III}(tpfc)] \rightarrow TP + [M^{II}(tpfc)]^- \quad (7)$$

$$TP^{\bullet -} + [M^{II}(tpfc)]^- \rightarrow TP + [M^{I}(tpfc)]^{2-} \quad (8)$$

The TEA radical cation reacts with a TEA molecule to form a carbon-centered radical ($E_{1/2} = -1.12$ V vs SCE in MeCN)[20] that can reduce $[M^{III}(tpfc)]$ but not $[M^{II}(tpfc)]^-$.

$$Et_3N^{\bullet +} + Et_3N \rightarrow Et_3NH^+ + Et_2N\dot{C}HCH_3 \quad (9)$$

$$Et_2N\dot{C}HCH_3 + [M^{III}(tpfc)] \rightarrow Et_2N^+{=}CHCH_3 + [M^{II}(tpfc)]^- \quad (10)$$

A pronounced difference between the photochemical reduction and the reduction by sodium and by electrochemistry lies in the fact that the photochemical process leads to production of acid (e.g., via reaction 9). As a result, reduced species such as $[M^{I}(tpfc)]^{2-}$ may undergo protonation. They may form a hydride and subsequently H_2 and may undergo hydrogenation on the macrocycle (as observed with porphyrins).[6−8,18]

$$[M^{I}(tpfc)]^{2-} + Et_3NH^+ \rightarrow [HM(tpfc)]^- + Et_3N \quad (11)$$

$$[HM(tpfc)]^- + Et_3NH^+ \rightarrow M^{III}(tpfc) + H_2 + Et_3N \quad (12)$$

Before photolysis, the absorption spectra of the corroles were first recorded in MeCN solutions. Addition of TEA resulted in a major change in the spectra. From comparison of the spectra recorded under these conditions to those recorded following reduction with sodium amalgam we conclude that TEA not only replaces the axial ligand but also reduces the metal center even under air. In the case of Ph_3PCo^{III}(tpfc), the spectrum of the starting material in MeCN exhibits two peaks at 374 and 406 nm of nearly equal intensities and after addition of TEA and equilibration for several minutes the spectrum has only one Soret peak at 412 nm corresponding to that of $[Co^{II}(tpfc)]^-$. (This solution was unstable under air and was slowly bleached, in contrast with the hexa-coordinated Co^{III} corroles with aromatic amines, which are air-stable and display Soret peaks of about 440 nm[17]). In the case of $ClFe^{IV}$(tpfc) and $ClFe^{IV}$(tdcc), addition of TEA led to immediate reduction of the compounds to the Fe^{III} corroles. These solutions were then photolyzed (after addition of TP and bubbling with Ar) and their spectra were recorded before photolysis and after different intervals of photolysis. Photoreduction of Fe^{III}(tpfc) and Fe^{III}(tdcc) led to formation of the Fe^{II} corroles. The spectra of the Fe^{II} and Co^{II} corroles were identical to those determined by reduction with sodium amalgam (Table 2).

Photoreduction of $[Fe^{II}(tpfc)]^-$, $[Fe^{II}(tdcc)]^-$, and $[Co^{II}(tpfc)]^-$ produced species with absorption spectra that are different from the spectra of the M^I corroles listed in Table 2. The main peaks for the Co(tpfc) product were at 408 and 587 nm (as compared with 408 and 574 nm for the Co^I-corrole). The peak positions shifted gradually upon photolysis and it is possible that Co^I-corrole is one of the intermediates in this process. On the other hand, the main peaks for the Fe(tpfc) product were at 407, 517, 556, 591, and 634 nm, i.e., quite different from those of the $[Fe^I(tpfc)]^{2-}$ listed in Table 2, indicating that the Fe^I complex is unstable under these conditions. At this stage, addition of O_2 led to substantial recovery of the Fe^{III}(tpfc). However, upon further photolysis (without O_2) the absorbance at all peaks decreased and then the solution became almost colorless; at this stage, no recovery of Fe^{III}(tpfc) was observed following addition of O_2, indicating degradation of the macrocycle.

Photochemical reduction in CO-saturated solutions led to different spectral changes. The first reduction product, $[Fe^{II}(tpfc)]^-$, strongly binds CO and the spectrum of the complex $[(CO)Fe^{II}(tpfc)]^-$, exhibits a very intense Soret peak at 403 nm and two small peaks at ≈530 and 553 nm (Figure 5). Extensive photolysis also led to bleaching. Similar results were obtained with Fe(tdcc) (but no spectral evidence was found for binding of CO to $[Co^{II}(tpfc)]^-$).

Photochemical reduction in CO_2-saturated solutions resulted in similar spectral changes to those found under Ar in the early stages of photolysis. When the photolysis was continued until nearly half the $[Fe^{II}(tpfc)]^-$ was reduced, a weak absorbance at 403 nm was observed, indicating partial formation of $[(CO)Fe^{II}(tpfc)]^-$. Continued photolysis produced large amounts of CO (see below).

Photolysis of He-saturated acetonitrile solutions containing TEA (5 vol %), TP (3 mmol L^{-1}), and either the cobalt or the iron corrole led to production of H_2, after a slight delay for the reduction of the starting material to the active species (Figures 6a and 7a). The maximal rate of H_2 production was similar with both Fe(tpfc) and Co(tpfc), $\approx 4 \times 10^{-7}$ mol L^{-1} s^{-1}. After several hours the production rate decreased and at longer times production of H_2 stopped. Photolysis of similar solutions saturated with CO_2 led to production of both H_2 and CO (Figures 6a and 7a). Both of these gases were produced at similar rates in the early stages of photolysis, after a slight delay, and the sum of [CO] + $[H_2]$ was slightly less than the $[H_2]$ produced under He. After several hours the rates of production of the two gases diverged; the ratio $[CO]/[H_2]$ was >1 for Co(tpfc) and <1 for Fe(tpfc), and at longer times production of the gases stopped. The results obtained with Fe(tdcc) (Figure 7b) are significantly different from those of Fe(tpfc) and Co(tpfc) in that the yield of CO in the early stages of photolysis was much higher than that of H_2 and higher than that found with the other corroles. This result is in line with the electrochemical experiments showing that Fe(tdcc) was a more efficient electrocatalyst for reduction of CO_2 than the other two corroles.

With 4.2×10^{-5} mol L^{-1} Co(tpfc) under CO_2, the total concentrations of both CO and H_2 reached a plateau after ≈10 h of photolysis. The plateau level of CO (4.2 mmol L^{-1}) was higher than that of H_2 (2.5 mmol L^{-1}). The results with similar concentrations of Fe(tpfc) and Fe(tdcc) under CO_2 were somewhat different; the yield of CO leveled off (at ≈2.2 mmol L^{-1}) but the yield of H_2 continued to rise (to >8 mmol L^{-1} with Fe(tpfc)). In contrast with the above results, production of H_2 in similar solutions under He reached a higher plateau level with Co(tpfc) (≈14 mmol L^{-1}) than with Fe(tpfc) (≈6 mmol L^{-1}).

As discussed above, H_2 is formed via reactions 11 and 12, and CO is formed via reactions 1 and 2. The finding with Co(tpfc) and Fe(tpfc) that the rates of production of the two gases are similar suggests that reaction with protons (reaction

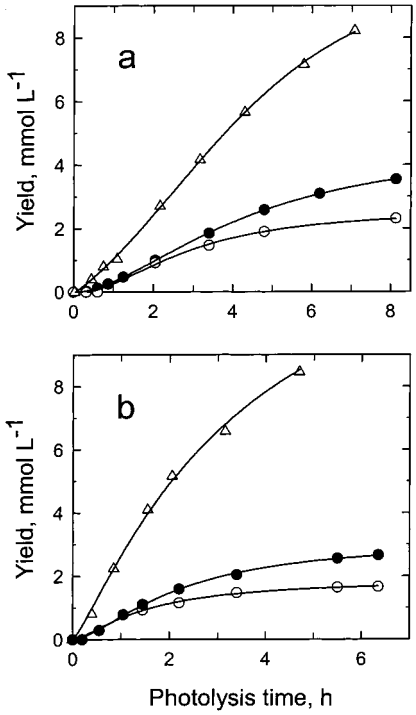

Figure 6. Photochemical production of CO and H_2 in MeCN solutions of cobalt corrole (a) and cobalt porphyrin (b). Production of H_2 (△) in He-saturated solution and production of CO (●) and H_2 (o) in CO_2-saturated solution. The solutions contained 5% TEA, 3 mmol L^{-1} TP, and (a) 4.2×10^{-5} mol L^{-1} Co^{III}(tpfc), (b) 5.2×10^{-5} mol L^{-1} Co^{II}-(TTP). The standard uncertainties are ±10%.

11) efficiently competes with reaction with CO_2 (reaction 1) despite the large excess of CO_2 over protons in the solution. With Fe(tdcc), however, the reaction with CO_2 predominates in the early stages of photolysis. In parallel with these reactions, the macrocycle undergoes hydrogenation. The partially hydrogenated complexes also catalyze the photochemical production of CO and H_2 but exhibit different reactivities. After very long irradiations, production of all gases stops. This may be due to decomposition of the metal complex into an unreactive product. An additional factor is the loss of TP as a sensitizer. The $TP^{\bullet-}$ radical anion transfers an electron to the metal complex to recover TP (e.g., reactions 8, 9). However, $TP^{\bullet-}$ also undergoes protonation to form $TPH^{\bullet}$ and this leads to loss of the sensitizer. We found that a considerable fraction of the TP was lost during these experiments and this loss was related to the termination of the photochemical production of the two gases. The loss of TP was estimated from the UV absorbance of the solution before and after photolysis. In those cases where the final yields were lower, the remaining TP concentration was quite low, indicating that the lack of TP limited the yield. In those cases where the final yields were higher, the remaining TP concentration was also higher, indicating that other factors limited the yield. Thus the end of the photochemical process is determined by a combination of several effects, as discussed before for the metalloporphyrins.[18]

For comparison of corroles to porphyrins, Figures 6b and 7c show the results obtained by photolysis of Fe(TTP) and Co(TTP) (TTP = tetrakis(3-methylphenyl)porphyrin)[21] under identical conditions (MeCN/TEA/TP, solute concentrations, cell size, photolysis source) to those used with the Fe and Co corroles (Figure 6a and 7a). For the Co corrole (Figure 6a) and porphyrin (Figure 6b), the yield of H_2 under He and the yields of H_2 and CO under CO_2 are each similar for the two complexes, within a factor of <2. The results with Fe(tpfc) (Figure 7a) are not

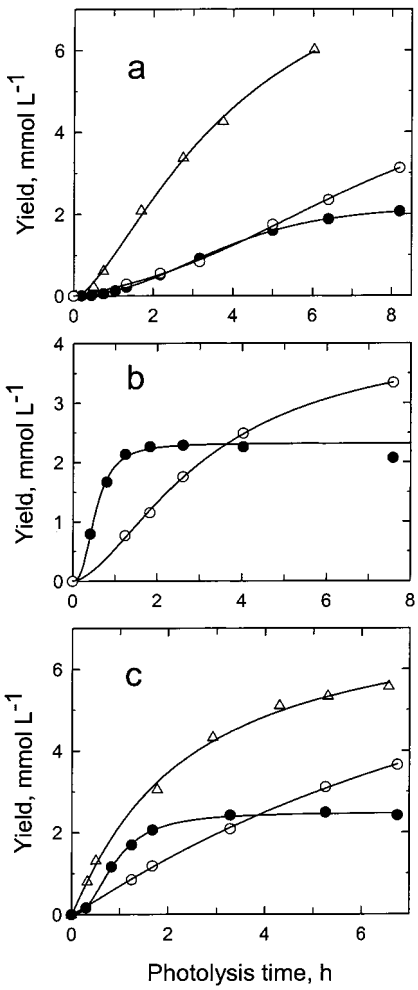

Figure 7. Photochemical production of CO and H_2 in MeCN solutions of iron corroles (a,b) and iron porphyrin (c). Production of H_2 (△) in He-saturated solution and production of CO (●) and H_2 (o) in CO_2-saturated solution. The solutions contained 5% TEA, 3 mmol L^{-1} TP, and (a) 4.8×10^{-5} mol L^{-1} $ClFe^{IV}$(tpfc), (b) 4.5×10^{-5} mol L^{-1} $ClFe^{IV}$-(tdcc), (c) 5.0×10^{-5} mol L^{-1} Fe^{II}(TTP). The standard uncertainties are ±10%.

very different from those of the Co complexes but the results with Fe(tdcc) (Figure 7b) are close to those obtained with Fe(TTP) (Figure 7c); both of the latter two complexes are more effective in CO production in the early stages of photolysis.

The total concentrations of CO and H_2 produced in these experiments, with both sets of metal complexes, were ≈300 times larger than the concentrations of the metal complexes. The total concentrations of CO produced were 50 to 100 times larger than the concentrations of the complexes. The findings that the results for the corroles are generally similar to those obtained with the corresponding porphyrin indicate that despite the fact that the corroles react with CO_2 in their M^I oxidation state while the porphyrins have to be reduced beyond the M^I state to react with CO_2, in both cases the reduced species are hydrogenated at the macrocycle and are deactivated to similar extents.

Acknowledgment. This research was supported in part by the Division of Chemical Sciences, Office of Basic Energy Sciences, U.S. Department of Energy; work at NIST under Contracts DE-AI02-95ER14565; and work at BNL under Contract DE-AC02-98CH10886. Work at the Technion was supported by the Israel Science foundation under Grant 368/00 and by the Petroleum Research Fund.

References and Notes

(1) Hawecker, J.; Lehn, J.-M.; Ziessel, R. *J. Chem. Soc., Chem. Commun.* **1985**, 56. Grant, J. L.; Goswami, K.; Spreer, L. O.; Otvos, J. W.; Calvin, M. *J. Chem. Soc., Dalton Trans.* **1987**, 2105. Craig, C. A.; Spreer, L. O.; Otvos, J. W.; Calvin, M. *J. Phys. Chem.* **1990**, *94*, 7957. Kelly, C. A.; Mulazzani, Q. G.; Venturi, M.; Blinn, E. L.; Rodgers, M. A. J. *J. Am. Chem. Soc.* **1995**, *117*, 4911.

(2) (a) Fujita, E.; Brunschwig, B. S.; Ogata, T.; Yanagida, S. *Coord. Chem. Rev.* **1994**, *132*, 195. (b) Ogata, T.; Yanagida, S.; Brunschwig, B. S.; Fujita, E. *J. Am. Chem. Soc.* **1995**, *117*, 6708. (c) Matsuoka, S.; Yamamoto, K.; Ogata, T.; Kusaba, M.; Nakashima, N.; Fujita, E.; Yanagida, S. *J. Am. Chem. Soc.* **1993**, *115*, 601. (d) Ogata, T.; Yamamoto, Y.; Wada, Y.; Murakoshi, K.; Kusaba, M.; Nakashima, N.; Ishida, A.; Takamuku, S.; Yanagida, S. *J. Phys. Chem.* **1995**, *99*, 11916.

(3) Fisher, B.; Eisenberg, R. *J. Am. Chem. Soc.* **1980**, *102*, 7361. Sullivan, B. P.; Bolinger, C. M.; Conrad, D.; Vining, W. J.; Meyer, T. J. *J. Chem. Soc., Chem. Commun.* **1985**, 1414. Beley, M.; Collin, J.-P.; Ruppert, R.; Sauvage, J.-P. *J. Am. Chem. Soc.* **1986**, *108*, 7461. Fujita, E.; Haff, J.; Sanzenbacher, R.; Elias, H. *Inorg. Chem.* **1994**, *33*, 4627.

(4) For reviews see: *Catalytic Activation of Carbon Dioxide*; Ayers, W. M., Ed.; ACS Symposium Series, Vol. 363, 1988. Behr, A. *Carbon Dioxide Activation by Metal Complexes*; VCH: Weinheim, 1988. *Electrochemical and Electrocatalytic Reactions of Carbon Dioxide*; Sullivan, B. P., Ed.; Elsevier: Amsterdam, 1993. Sutin, N.; Creutz, C.; Fujita, E. *Comments Inorg. Chem.* **1997**, *19*, 67.

(5) Hammouche, M.; Lexa, D.; Savéant, J.-M.; Momenteau, M. *J. Electroanal. Chem. Interfacial Electrochem.* **1988**, *249*, 347. Hammouche, M.; Lexa, D.; Momenteau, M.; Savéant, J.-M. *J. Am. Chem. Soc.* **1991**, *113*, 8455. Bhugun, I.; Lexa, D.; Savéant, J.-M. *J. Am. Chem. Soc.* **1994**, *116*, 5015. Bhugun, I.; Lexa, D.; Savéant, J.-M. *J. Am. Chem. Soc.* **1996**, *118*, 1769.

(6) Grodkowski, J.; Behar, D.; Neta, P.; Hambright, P. *J. Phys. Chem. A* **1997**, *101*, 248.

(7) Behar, D.; Dhansekaran, T.; Neta, P.; Hosten, C. M.; Ejeh, D.; Hambright, P.; Fujita, E. *J. Phys. Chem.* **1998**, *102*, 2870.

(8) Grodkowski, J.; Dhanasekaran, T.; Neta, P.; Hambright, P.; Brunschwig, B. S.; Shinozaki, K.; Fujita, E. *J. Phys. Chem. A* **2000**, *104*, 11332.

(9) (a) Kadish, K. M.; Koh, W.; Tagliatesta, P.; Sazou, D.; Paolesse, R.; Licoccia, S.; Boschi, T. *Inorg. Chem.* **1992**, *31*, 2305. (b) Van Caemelbecke, E.; Will, S.; Autret, M.; Adamian, V. A.; Lex, J.; Gisselbrecht, J.-P.; Gross, M.; Vogel, E.; Kadish, K. M. *Inorg. Chem.* **1996**, *35*, 184. (c) Kadish, K. M.; Adamian, V. A.; Van Caemelbecke, E.; Gueletii, E.; Will, S.; Erben, C.; Vogel, E. *J. Am. Chem. Soc.* **1998**, *120*, 11986.

(10) Gross, Z.; Simkhovich, L.; Galili, N. *J. Chem. Soc., Chem. Commun.* **1999**, 599. Meier-Callahan, A. E.; Gray, H. B.; Gross, Z. *Inorg. Chem.* **2000**, *39*, 3605.

(11) The mention of commercial equipment or material does not imply recognition or endorsement by the National Institute of Standards and Technology, nor does it imply that the material or equipment identified are necessarily the best available for the purpose.

(12) Simkhovich, L.; Galili, N.; Saltsman, I.; Goldberg, I.; Gross, Z. *Inorg. Chem.* **2000**, *39*, 2704.

(13) Riddick, J. A.; Bunger, W. B.; Sakano, T. K. *Organic Solvents, Physical Properties and Methods of Purification*, 4th ed.; Wiley: New York, 1986.

(14) Simkhovich, L.; Mahammed, A.; Goldberg, I.; Gross, Z. *Chem. Eur. J.* **2001**, *7*, 1041.

(15) Fuhrhop, J.-H.; Kadish, K. M.; Davis, D. G. *J. Am. Chem. Soc.* **1973**, *95*, 5140.

(16) It is a known phenomenon that many Co^{III} porphyrins in the solid state contain varying amounts of Co^{II} porphyrins, depending on the method of preparation and drying.

(17) Mahammed, A.; Giladi, I.; Goldberg, I.; Gross, Z. *Chem. Eur. J.* **2001**, *7*, 4259.

(18) Dhanasekaran, T.; Grodkowski, J.; Neta, P.; Hambright, P.; Fujita, E. *J. Phys. Chem. A* **1999**, *103*, 7742.

(19) Matsuoka, S.; Kohzuki, T.; Pac, C.; Ishida, A.; Takamuku, S.; Kusaba, M.; Nakashima, N.; Yanagida, S. *J. Phys. Chem.* **1992**, *96*, 4437.

(20) Wayner, D. D. M.; McPhee, D. J.; Griller, D. *J. Am. Chem. Soc.* **1988**, *110*, 132. Armstrong, D. A.; Rauk, A.; Yu, D. *J. Am. Chem. Soc.* **1993**, *115*, 666.

(21) Further details on metalloporphyrins were presented in refs 7 and 18.